

Thermodynamic and magnetic properties of metastable $\text{Fe}_x\text{Cu}_{100-x}$ solid solutions formed by mechanical alloying

E. Ma^{a)} and M. Atzmon

Department of Nuclear Engineering, The University of Michigan, Ann Arbor, Michigan 48109-2104

F. E. Pinkerton

Physics Department, General Motors Research and Environmental Staff, Warren, Michigan 48090-9055

(Received 20 July 1992; accepted for publication 20 March 1993)

Metastable solid solutions of Fe and Cu, which are immiscible in equilibrium, have been formed using high-energy ball milling of elemental powder mixtures. Single-phase face-centered-cubic (fcc) solid solution was obtained for $0 < x < 60$, and body-centered-cubic (bcc) solid solution for $75 < x < 100$. The transition from fcc to bcc occurred near $x = 70$, where a mixture of fcc and bcc phases was obtained. The enthalpy of transformation to equilibrium was measured using differential scanning calorimetry. The average atomic volume of the phases exhibits a positive deviation from Vegard's law, in qualitative agreement with the large positive enthalpy of mixing in this system. The magnetic moments and Curie temperatures for the metastable solid solutions have been determined and compared with those reported for Fe-Cu alloys formed by vapor deposition. Calculations of the formation enthalpy (ΔH) and free energy (ΔG) have been performed based on CALPHAD data, with corrections based on our magnetization measurements. The calculated ΔG results are used to explain the observed fcc-bcc transition under polymorphous constraints.

I. INTRODUCTION

Metastable alloys offer a variety of new properties and applications. There has been long-standing interest in new preparation techniques and novel properties of nonequilibrium alloys.¹ A number of studies have been carried out in the Fe-Cu system,²⁻⁶ which has negligible mutual solid solubility in equilibrium at temperatures below 700 °C.⁷ The primary aims have been to investigate the possibility of forming metastable phases in such a system with large positive enthalpy of mixing ($\Delta H_{\text{mix}} = +13$ kJ/mol for $\text{Fe}_{50}\text{Cu}_{50}$ according to the Miedema model⁸) and to study the alloying effect on the magnetism of transition metals. Metastable solid solutions have been produced successfully by vapor deposition²⁻⁴ and by ion beam mixing⁵ in this system. In recent years, mechanical alloying has emerged as an alternative technique of producing metastable alloys.⁹ It has the advantages of low-temperature processing, easy control of compositions, and the production of relatively large amount of samples. These greatly facilitate the characterization and application of the resulting metastable alloys. It is therefore of interest to exploit this alternative technique to synthesize and characterize nonequilibrium alloys in the Fe-Cu system.

The objectives of the present article are twofold. First, we show that high-energy ball milling of elemental powders can be used to alloy the immiscible iron and copper to form metastable solid solutions. We compare the structural and magnetic properties of these metastable solutions with those of the same alloys formed by vapor deposition and explore possible property differences associated with the preparation technique. The second objective, which is the

emphasis of this article, is to characterize the thermodynamic functions of metastable Fe-Cu solid solutions. Such a characterization, which is of primary importance to understanding the formation and stability of these nonequilibrium solid solutions, has not been reported so far, although considerable work exists for equilibrium phases in this system. We will present and compare the results from both experiments and calculations. The calorimetric measurement of transformation enthalpies is possible due to the easy preparation of relatively large quantity of metastable solutions by mechanical alloying. Our measurements of magnetic properties allows the incorporation of magnetic contributions to the thermodynamic functions. The calorimetric data will be compared with model calculations.

II. EXPERIMENTS

Mechanical alloying was performed using a SPEX 8000 laboratory miller/mixer. 8 g of commercial Fe (−325 mesh, 99.9% purity) and Cu (−100 mesh, 99.9% purity) powder mixture and hardened stainless-steel balls were loaded in Ar atmosphere into a hardened stainless-steel vial at a ball to powder weight ratio of 4:1. The powder blends had overall compositions $\text{Fe}_x\text{Cu}_{100-x}$, with x (in at. %) ranging from 0 to 100. The milling duration varied from 12 to 40 h, with typical runs lasting 20 h. The vial temperature was maintained at approximately 35 °C using a cooling fan. The milled samples were analyzed using x-ray diffraction (XRD) and differential scanning calorimetry (DSC) in a Perkin Elmer DSC-7 calorimeter. DSC samples were sealed in Au pans to allow temperature excursions to 730 °C. The baseline was determined by repeating each run without disturbing the sample, and subtracted from the signal recorded during the original run.

^{a)}Present address: Mechanical Engineering Department, LSU, Baton Rouge, LA 70803.

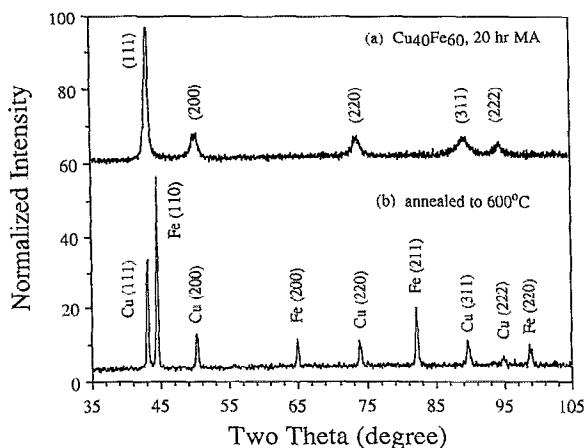


FIG. 1. X-ray diffraction patterns for (a) 20 h ball-milled $\text{Fe}_{60}\text{Cu}_{40}$ powder, showing the presence of a single fcc phase; and (b) the same powder as in (a) after annealing to 600 °C, showing phase separation into terminal Fe and Cu phases.

Magnetization measurements were performed using two instruments: (1) a superconducting quantum interference device (SQUID), Quantum Design MPMS, was used below 55 °C, and (2) a Princeton Applied Research Model 155 vibrating sample magnetometer (VSM) was used in conjunction with (i) a 9 T superconducting magnet at room temperature and below and (ii) 1.9 electromagnet above room temperature.

III. RESULTS AND DISCUSSION

A. Phase transformation

As an example, Fig. 1(a) shows an XRD pattern for a ball-milled $\text{Fe}_{60}\text{Cu}_{40}$ sample. The pattern suggests that only one face-centered-cubic (fcc) phase is present. All the fcc diffraction peaks in the pattern are slightly displaced from their positions for elemental Cu. The body-centered-cubic (bcc) Fe diffraction peaks, which were prominent in the XRD pattern for the $\text{Fe}_{60}\text{Cu}_{40}$ powder mixture before ball milling, have disappeared. These indicate alloying of Fe and Cu, forming a single fcc solid solution. The small shifts in fcc peak positions upon alloying are consistent with the similar atomic sizes of Fe and Cu. Further proof of alloying is provided by the measured magnetic properties presented in the next section. The equilibrium Fe-Cu phase diagram predicts negligible metal solid solubility at temperatures below 700 °C.⁷ After annealing the ball-milled sample in DSC to 600 °C, Bragg peaks corresponding to the nearly pure elemental fcc and bcc terminal phases become evident in the x-ray diffraction pattern of Fig. 1(b), indicating that the single fcc phase obtained after milling has transformed back to equilibrium. This phase transformation is accompanied by a heat release over a broad temperature range from about 300 to 500 °C, as shown in the DSC trace of Fig. 2. Since the entropic contribution to the free energy is relatively small (see below), this exothermic transformation is consistent with the notion that the as-milled sample is in a metastable state with respect to terminal Fe and Cu.

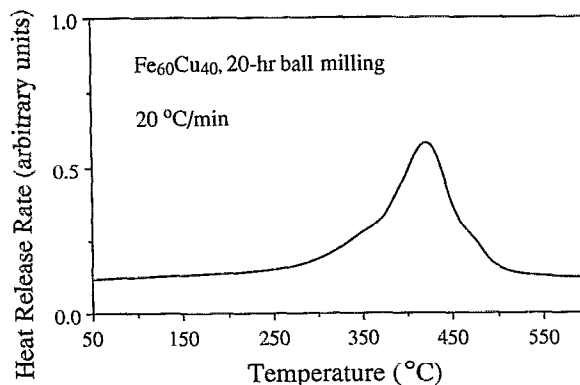


FIG. 2. DSC trace, at 20 °C/min, of 20 h ball-milled $\text{Fe}_{60}\text{Cu}_{40}$ powder, showing the heat release during phase decomposition.

Single-phase metastable $\text{Fe}_x\text{Cu}_{100-x}$ solid solutions were also obtained for other compositions after 20–40 h of ball milling. The product phase was fcc for $0 < x < 60$, and bcc for $75 < x < 100$. For $65 < x < 75$, both the fcc and the bcc phases were present. Similar results have been obtained in this system by various authors in recent years. Sumiyama and Nakamura, using rf sputtering, produced films of Fe-Cu solid solutions, with fcc structure for $0 < x < 40$, bcc for $60 < x < 100$, and a mixture of fcc and bcc for the central composition range, $x = 40-60$.³ Chien *et al.* prepared films of solid solutions using magnetron dc sputtering, and observed fcc solid solutions for $0 < x < 60$ and bcc for $75 < x < 100$, with both phases observed for $x = 60-75$.⁴ There have also been attempts to form Fe-Cu solid solutions using mechanical alloying. Shingu *et al.* used a low-energy ball milling technique and obtained Fe-Cu solid solutions after 400 h: fcc for $0 < x < 60$, and bcc for $x > 70$.⁶ Recently, in an independent study of the Fe-Cu system using high-energy ball milling, Eckert *et al.*¹⁰ found fcc solution with x up to 60, and bcc with $x > 80$. A coexistence region was observed in the range of $60 < x < 80$. Our observations (fcc for $x < 60$, bcc for $x > 75$, two-phase mixture for $x = 60-75$) agree well with these findings.

In Fig. 3, we show a plot of the average atomic volume of the solution phase, calculated from the lattice parameters determined from the x-ray diffraction data, as a function of composition. An obvious positive deviation from Vegard's law for ideal solutions,¹¹ up to about 2%, is observed. This is qualitatively consistent with the large positive enthalpy of mixing of this alloy system (see below).¹¹ The lattice parameters of the bcc alloys are similar to those observed previously by various authors for vapor-deposited bcc films,²⁻⁴ while those for the fcc alloys are apparently larger for our ball-milled samples than for deposited films. Again, our lattice parameter data agree particularly well with those for high-energy ball-milled alloys obtained by Eckert *et al.*¹⁰ Those observed by Shingu *et al.* are also similar. The observed continuous and monotonic change of the lattice parameters as a function of composition provides additional evidence that the ball-milled solid solutions consist of a single phase. Deviation from the overall nominal composition is possible and difficult to measure

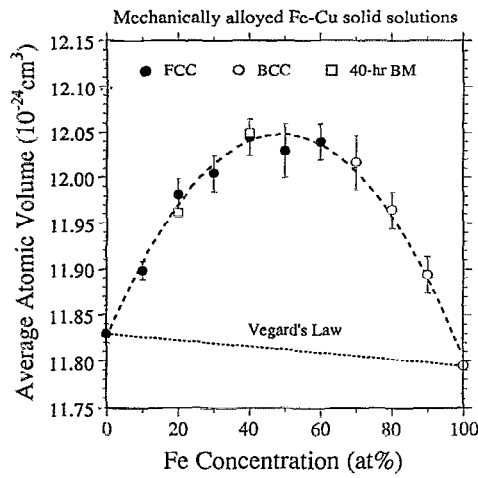


FIG. 3. Average atomic volume as a function of Fe concentration, calculated from lattice parameters determined by x-ray diffraction data, of the fcc (filled circles) and bcc (open circles) Fe-Cu solid solutions formed by 20 h ball milling. Data for 40 h milled samples at selected compositions are also included (squares). The dotted line is that calculated for an ideal solution.

quantitatively, but is unlikely to be very significant. This point will be further discussed in Sec. III B in the context of magnetic properties.

We determined the enthalpy of formation of the metastable solutions by integrating the heat release measured during heating of the as-milled powders in the DSC at 20 °C/min to 600–730 °C. X-ray diffraction confirmed that the metastable alloys transformed back to equilibrium, i.e., terminal Fe and Cu phases, during this process [e.g., see Fig. 1(b)]. This transformation was completed at temperatures ranging from 500 to 730 °C, depending on the alloy composition. The total enthalpy obtained by integration is

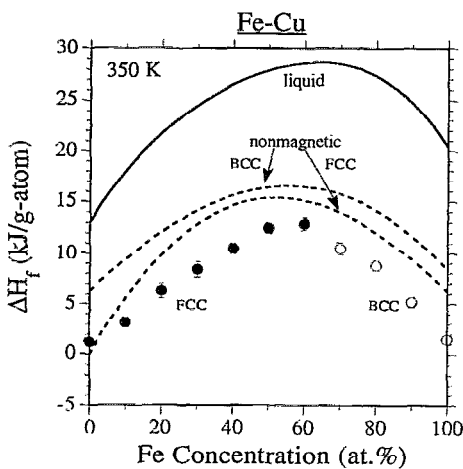


FIG. 4. Measured enthalpies of transformation of the metastable fcc (filled circles) and bcc (open circles) Fe-Cu solid solutions as a function of Fe concentration. These data are used to approximate the enthalpies of formation (ΔH) to compare with calculated ΔH vs x curves for paramagnetic fcc and bcc solutions (dashed curves). The calculated enthalpy for an undercooled liquid is shown with a solid curve. The calculations are based on the CALPHAD data of Ref. 19.

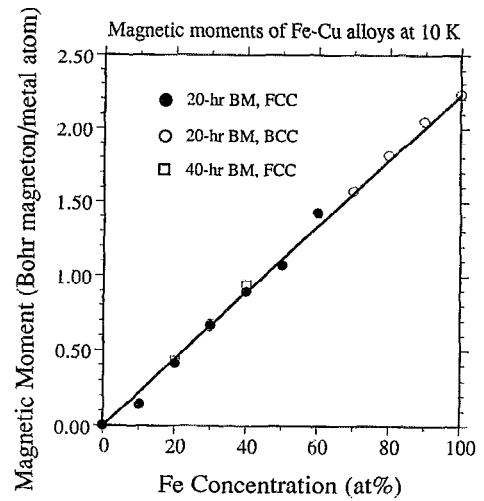


FIG. 5. Magnetic moment σ , in μ_B /metal atom, measured at 10 K, vs x for fcc (filled circles) and bcc (open circles) Fe-Cu solid solutions formed by ball milling. Data for 40 h milled samples have also been included (squares).

plotted in Fig. 4 (filled and open circles) as a function of x . These transformation enthalpy data are in excellent quantitative agreement with those of Eckert *et al.*,¹⁰ who measured the same quantity by heating the samples in DSC to 600 °C. Although this latter temperature is not sufficiently high for some compositions for a complete transformation to take place, the heat release above 600 °C is only a small portion of that of the entire transformation process.

The fact that our measured lattice parameters and transformation enthalpies (Figs. 3 and 4) are in good agreement with the results of a parallel ball milling study of the Fe-Cu system by Eckert *et al.*¹⁰ suggests good reproducibility of these metastable alloys and their properties by high-energy ball milling. We may therefore refer to Ref. 10 for additional information on ball-milled Fe-Cu that are not obtained in this study. For example, using transmission electron microscopy and electron diffraction, Eckert *et al.* confirmed the formation of single-phase solid solutions. They also carried out a detailed characterization of the grain size and lattice strain as a function of composition and ball-milling duration. In this article, we will concentrate on the two main contributions of this work: (i) measurements of the magnetic properties of these solid solutions, and (ii) the calculation of the thermodynamic functions of these phases, incorporating magnetic contributions, to compare with experimental results and to explain the observed fcc-bcc transition.

B. Magnetic measurements

Magnetic properties of vapor-deposited metastable Fe-Cu alloys have been the subject of several previous publications.^{2–4} Most of the Fe-Cu alloys we obtained by ball milling also appeared to be ferromagnetic at room temperature. We have measured the saturation magnetization of the alloys and the Curie temperature, T_c , to compare with results for deposited films. The saturation magnetization was measured at 10 K in a field of 55 kG. Figure 5 displays

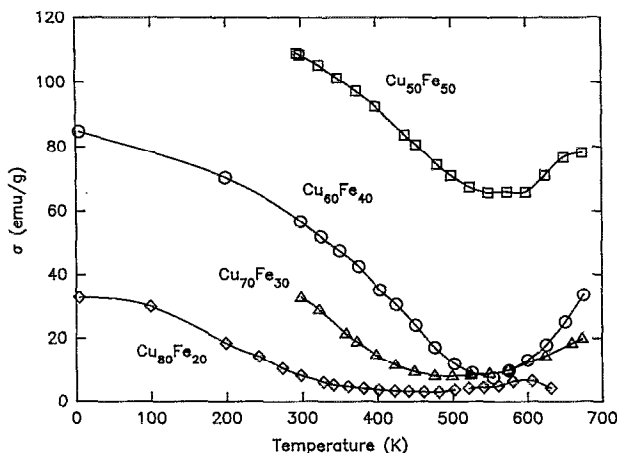


FIG. 6. Magnetic moment σ , in emu/g, as a function of temperature for 40 h ball-milled $\text{Fe}_x\text{Cu}_{100-x}$ fcc solid solutions ($x=20, 30, 40, 50$).

the low-temperature saturation magnetization data. In Fig. 5, the magnetic moment σ , in units of Bohr magneton per metal atom ($\mu_B/\text{metal atom}$), is plotted versus Fe concentration. The data nearly coincide with a straight interpolation line, which would be the results for simple magnetic dilution. Very similar results have been obtained for fcc Fe-Cu alloys prepared by vapor deposition.²⁻⁴ The observed linear relationship has been shown to contrast with the behavior of many other binary alloys of Fe and a non-magnetic element, where the Fe moment vanishes at a finite Fe concentration of about 40–60 at. %.⁴ For selected compositions, we have measured the magnetic moment, as well as lattice parameters and enthalpy of transformation, for different milling durations. No significant variation was observed for milling between 20 and 40 h.

The Curie temperatures, T_c , for the deposited bcc and fcc solid solutions have been determined by Sumiyama and Nakamura³ and by Chien *et al.*⁴ However, since the lattice parameters they report for the fcc solutions differ from those in the present study, we have carried out a systematic measurement of the Curie temperatures of the ball-milled fcc solid solutions. Figure 6 displays measured magnetic moment, σ , in units of emu/g ($1 \text{ emu} = 1.078 \times 10^{20} \mu_B$), of ball-milled $\text{Fe}_x\text{Cu}_{100-x}$ ($x=20, 30, 40, 50$) powders as a function of temperature. It is seen that the magnetization of the fcc phase drops with increasing temperature in a fashion consistent with that of ferromagnets. The Curie temperatures T_c have been rigorously determined for these compositions using plots of σ^2 vs H/σ at each temperature (Arrot plots).¹² This standard technique relies on the linearity of σ^2 vs H/σ at large applied fields. At $T = T_c$, linear extrapolation of the high-field response to $H/\sigma = 0$ passes through the origin. The increase of magnetization seen at higher temperatures is indicative of the decomposition of the fcc solid solution into nearly pure fcc Cu and bcc Fe ($T_c = 1043 \text{ K}$). For solutions with $x > 60$, we did not attempt to determine T_c because it becomes significantly higher than the temperature at which phase decomposition is observed to begin (typically around 500 K for low heating rates). The measured T_c values for our fcc solutions

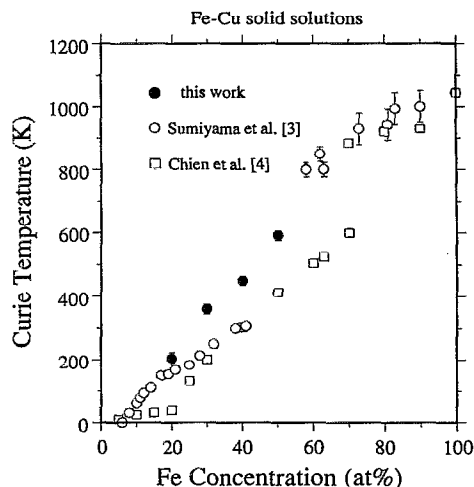


FIG. 7. Curie temperature, T_c , vs x for ball milled Fe-Cu fcc solid solutions (filled circles). Data for vapor deposited fcc and bcc solutions from the literature^{3,4} have been included for comparison.

are shown as a function of Fe concentration in Fig. 7, together with the results reported for vapor-deposited fcc and bcc films.^{3,4} For the fcc solutions, the magnitudes of the Curie temperatures for ball-milled powder are systematically higher than those for deposited films. As mentioned above, a difference in lattice parameters has also been noticed for fcc solutions prepared by the two different methods.

The measured magnetic properties provide additional evidence that alloying Fe and Cu has indeed taken place during the ball milling process. As can be seen in Fig. 6, T_c values measured for several alloys are much lower than that for pure bcc Fe ($T_c = 1043 \text{ K}$). The magnetic moment, σ , drops down close to zero near T_c , indicating that residual pure bcc Fe cannot be present at concentrations higher than a few percent. It is also unlikely that pure Fe is present in the fcc structure, because pure fcc Fe and Cu would not exhibit the magnetic moment shown in Fig. 5. An fcc phase is magnetic only when Fe and Cu are alloyed. However, it is difficult to determine the small-scale compositional uniformity in these milled Fe-Cu alloys. Although smooth and continuous change of lattice parameter as a function of the overall composition (Fig. 3) is observed, some distribution of composition in the final milling product cannot be ruled out. In fact, at low temperature σ seems to decrease rather steeply with temperature. This could be explained as resulting from distributions of Curie temperatures due to residual compositional heterogeneity in the powders after milling.

C. Thermodynamic functions

Calculation of thermodynamic functions of metastable alloys has been a very difficult problem, especially in a magnetic system. In recent years, the semi-empirical CALPHAD method,¹³ which had been applied successfully to equilibrium alloys, had been extended to metastable regimes. CALPHAD uses analytical expressions, fit to experi-

mental equilibrium data, to describe the enthalpy and free energy of various phases in a binary system. In the general formalism, the free energy of a certain phase in a binary system is usually assumed to be described by

$$G = G_1x_1 + G_2x_2 + RT(x_1 \ln x_1 + x_2 \ln x_2) + G_{\text{ex}}, \quad (1)$$

where G_1 and G_2 are the free energies for the pure elements, x_1 and x_2 , the molar fraction of the components, T the absolute temperature, and G_{ex} the excess free energy of mixing. G_1 and G_2 are described by polynomials in T , and G_{ex} , by polynomials in x and T . These polynomials are derived from models, with coefficients obtained from numerical fits to known equilibrium data. The enthalpy and entropy functions (H and S , respectively) can be obtained by taking appropriate derivatives with respect to T (see below). In many cases, polynomials are derived and given for ΔG , the free energy difference between the phase in question and the reference phase(s). These polynomials are sometime taken to be first order in T , in which case ΔH and ΔS are assumed to be independent of T and are then easily determined from ΔG . For metastable phases, extrapolations of these expressions, determined for the equilibrium phases, are used as a first approximation. This methodology will be adopted in this article. Although CALPHAD is mostly empirical, we believe that its application in this case is worthwhile because (i) it is known that CALPHAD can provide useful information on the thermodynamic functions for metastable alloys; (ii) it has not been tested experimentally for metastable Fe-Cu solid solutions, and (iii) we are not aware of published first-principle total energy calculations, or other reliable calculations, for Fe-Cu alloys.

CALPHAD fitting for equilibrium Fe-Cu phases has been performed by a number of authors.¹⁴⁻¹⁹ We chose to use the most recent of these, the work published by Chuang *et al.*,¹⁹ since it has been shown to yield satisfactory agreement with the experimental phase diagram, and more importantly, since it has given analytic formulations of the magnetic contributions to the thermodynamic functions. We will first discuss the enthalpy of formation, ΔH , because a direct comparison can be made with experimental data. In the next paragraph, we will show that ΔH can be approximated by the transformation enthalpy data directly measured in our experiments (Fig. 4). Our experimental ΔH data for the metastable phases (Fig. 4) supply new input to evaluate the model calculations in the metastable regime.

As mentioned above, the transformations of milled powders back to equilibrium were completed in the DSC at temperatures < 700 °C. At such temperatures, the resulting equilibrium terminal phases have negligible solubility. Therefore, the measured transformation enthalpy closely approximates the enthalpy of formation from the elements, ΔH . Qualitatively, the measured ΔH values are positive, in agreement with the immiscibility of the binary system. However, these values include the energy stored in the crystals due to cold work during milling. During heating in the PSC, this stored energy is released mainly through grain growth and strain relief, the magnitude of which can

be estimated as follows: from Fig. 4, it is seen that approximately 1 kJ/mol has been stored in pure Fe or Cu. The grain sizes of the solutions are similar to those of the pure elements Fe and Cu (10–20 nm).¹⁰ The energy release due to grain growth is thus likely to be comparable to that for the pure elements, on the order of < 1 kJ/mol. The maximum rms strain observed for Fe-Cu solutions was reported to be about 0.3%.¹⁰ Such a strain level is relatively low compared with other ball-milled alloys (up to 3%).²⁰ The strain energy contribution, u , can be estimated using $u = Y/2\langle e^2 \rangle$,²¹ where Y is Young's modulus and $\langle e^2 \rangle^{1/2}$ is the rms strain. For typical values of $Y < 200 \times 10^9$ N/m² (e.g., for Cu, Y is about 130 GN/m²),²¹ an rms strain of 0.3% would only give an enthalpy of less than 0.01 kJ/mol. One concludes that the strain energy introduced by mechanical deformation is insignificant in the Fe-Cu case (note that strain energy will be on the order of 1 kJ/mol in other systems in which a rms strain of a few percent is observed). The above considerations of the grain boundary and strain energy contributions lead us to conclude that the stored energy in all the Fe-Cu alloys is likely to be close to the value of 1 kJ/mol observed for pure elements Fe and Cu. The error in ΔH due to cold work is therefore relatively small compared with the magnitude of ΔH (13 kJ/mol for $x = 50$), and will also be shown to be minor in our comparison with the CALPHAD extrapolations (see below), which contain relatively large error.

In Fig. 4, we have shown the calculated ΔH vs x curves at 350 K for the liquid (solid curve), as well as for the paramagnetic fcc and bcc solutions (dashed curves). These curves have been calculated using direct extrapolation in composition and temperature of the CALPHAD expressions of Chuang *et al.* for nonmagnetic solid solutions.^{19,22} These calculated curves can be compared with experimental ΔH data (circles) shown in the same figure. It is apparent that both calculated curves for paramagnetic fcc and bcc solid solutions are appreciably higher than the experimental data. However, it is well known that bcc Fe is ferromagnetic at room temperature, and in fact, most of the solutions we obtained are magnetic (Fig. 7). Therefore, the magnetic contribution to ΔH needs to be taken into account in order to obtain a meaningful comparison. In the original work of Chuang *et al.*,^{19,22} a magnetic term is an indispensable addition to the CALPHAD calculation in order to properly describe magnetic bcc Fe and the corresponding terminal solution at low temperatures.

Chuang *et al.* determined the expression for the magnetic contribution to the thermodynamic functions by first deducing an analytic expression for the magnetic specific heat. The tabulated experimental specific heat was considered to be a combination of the lattice (including the correction due to the dilation of the lattice), electron, and magnetic contributions. The first two contributions, calculated using established models, were subtracted from the experimental specific heat to give the "experimental" magnetic specific heat. An empirical mathematical expression (see next paragraph) was then proposed to describe the magnetic specific heat, and the parameters in this equation were determined from a constrained least-squares fit to the

experimental magnetic specific heat data. This analytic expression was then used to calculate magnetic entropy, enthalpy, and Gibbs free energy. The magnetic contribution was added to the CALPHAD expressions for nonmagnetic phases, to yield thermodynamic functions and a phase diagram. These calculations were found to yield excellent agreement with experimental equilibrium data for both pure magnetic elements (Fe, Ni, Co) and for Fe-Cu equilibrium alloys. Based on their calculations, Chuang *et al.* pointed out that had Fe not been magnetic, the fcc state would be the ground state. In other words, it is the subtle magnetic effects that shift the ground state of Fe from fcc to bcc.

Chuang *et al.* expressed the magnetic contribution to ΔH and ΔG as a function of the magnetic moment and the Curie temperature, the two quantities measured in our experiments (Figs. 5–7). For the $\text{Fe}_x\text{Cu}_{100-x}$ alloy with saturation magnetization σ and Curie temperature T_c , the magnetic contribution to ΔG at temperature T , i.e., the free-energy difference between the completely paramagnetic state (cpm) and the equilibrium magnetic state (eqm), was expressed as^{19,22}

$$\Delta G^{\text{cpm} \rightarrow \text{eqm}} = -\frac{k_p T_c}{(8p)^2} \exp\left[8p\left(1 - \frac{T}{T_c}\right)\right] \quad (T_c < T), \quad (2a)$$

$$\Delta G^{\text{cpm} \rightarrow \text{eqm}} = -\frac{(1+8p)}{(8p)^2} k_p T_c + \left(\frac{k_f}{4} + \frac{k_p}{8p}\right) T - \frac{k_f T_c}{16} \left[3 + \exp\left[-4\left(1 - \frac{T}{T_c}\right)\right]\right] \quad (T < T_c), \quad (2b)$$

where $k_p = 2.28R[0.96 + (1-x)]\ln[\sigma + 1]$ with δ in μ_B/atom , $k_f = 1.28k_p$, R the gas constant, $p=1$ for bcc, and $p=2$ for fcc. For details of the formulation of $\Delta G^{\text{cpm} \rightarrow \text{eqm}}$, the readers are referred to Refs. 19 and 22. Based on Eqs. (2),^{19,22} we have also derived expressions for the magnetic entropy and enthalpy using

$$\Delta S^{\text{cpm} \rightarrow \text{eqm}} = -\frac{\partial \Delta G^{\text{cpm} \rightarrow \text{eqm}}}{\partial T} \quad (3)$$

and

$$\Delta H^{\text{cpm} \rightarrow \text{eqm}} = \Delta G^{\text{cpm} \rightarrow \text{eqm}} + T \Delta S^{\text{cpm} \rightarrow \text{eqm}}. \quad (4)$$

We obtain for the magnetic contribution to ΔH

$$\Delta H^{\text{cpm} \rightarrow \text{eqm}} = -\frac{k_p T_c}{(8p)^2} \left(1 + 8p \frac{T}{T_c}\right) \times \exp\left[8p\left(1 - \frac{T}{T_c}\right)\right] \quad (T_c < T), \quad (5a)$$

$$\Delta H^{\text{cpm} \rightarrow \text{eqm}} = -\frac{(1+8p)}{(8p)^2} k_p T_c - \frac{k_f T_c}{16} \left[3 + \left(1 - 4 \frac{T}{T_c}\right)\right] \times \exp\left[-4\left(1 - \frac{T}{T_c}\right)\right] \quad (T < T_c). \quad (5b)$$

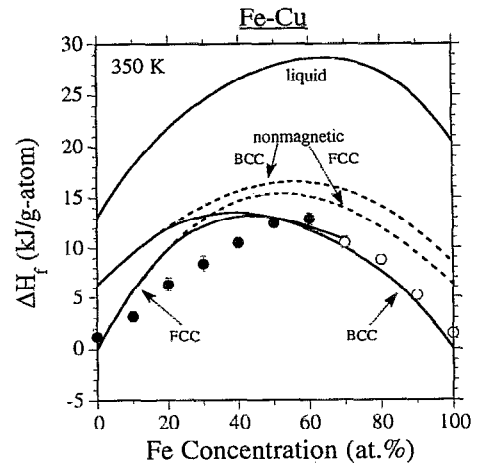


FIG. 8. ΔH vs x curves for fcc and bcc Fe-Cu solid solutions after incorporating magnetic contributions (solid curves). Curves for nonmagnetic solutions (dashed, from Fig. 4) are also included. The experimental ΔH data (circles) are the same as in Fig. 4.

In our calculations, we have applied Chuang's magnetic terms, because (i) they were an integral part of their original formulation of the Fe-Cu system; (ii) they were derived from models based on experimental data; and (iii) they have been proven to be successful for equilibrium elemental and Fe-Cu phases. These terms, however, cannot be simply extrapolated in composition and temperature, because of the unknown variation of the magnetic properties of the specific alloy has been given in Eq. (2). We are thus able to apply Eq. (2) to calculate the magnetic contributions using our measured data for magnetic properties of these metastable solutions. For the ball-milled fcc solutions, we have used our measured T_c values in the calculations. T_c for $x > 60$ could not be measured in our experiments because it is too far above the phase-decomposition temperature, so we estimated the values from previously obtained data (Fig. 7). In Fig. 8, the calculated magnetic terms have been added to the paramagnetic solution curves (dashed curves) of Fig. 4 to give the modified curves for the magnetic solid solutions (solid curves). Good agreement with the experimental data is achieved for the bcc solution. For the fcc phase, however, agreement is satisfactory only at near-equiatomic compositions. Considerable discrepancies still exist for Cu-rich fcc solutions.

This existing discrepancy is, in fact, not surprising. We note that we do not expect a perfect match with experiments using the CALPHAD approach. This is because CALPHAD expressions, which are derived based on fitting to limited equilibrium data, are expected to introduce errors when extrapolated deeply into metastable regimes.^{23,24} In fact, Fe and Cu have very limited solid solubility even at high temperatures (e.g., the Fe solubility in fcc Cu has a maximum of about 5 at. % at 1095 °C). Although the current free-energy expressions yield a good match with equilibrium data, they become inappropriate when extrapolated deeply into metastable composition/temperature

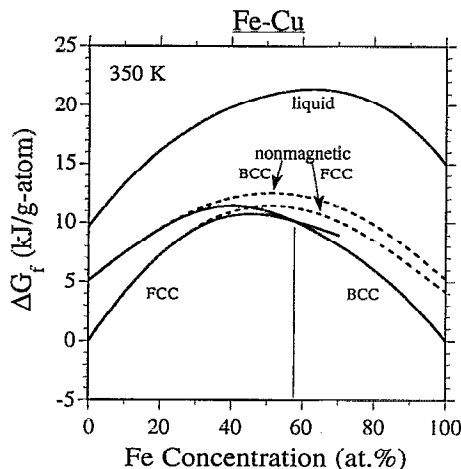


FIG. 9. Free energy (ΔG) vs x curves for nonmagnetic (dashed curves) and magnetic (solid curves) fcc and bcc Fe-Cu solid solutions. Note that the two solid curves intersect at approximately $x=60$.

regimes using the fitting parameters derived only for narrow equilibrium regimes. Thus, the magnetic term is not the only source of error. In fact, for the Cu-rich fcc solutions, the modeling of the magnetic term is unlikely to be the main source of error, since the magnetization of these solutions is relatively small to begin with. Although imperfect, the CALPHAD results are useful, as evidenced by the good agreement found for the bcc phase. The observed discrepancy for the fcc phase (up to 2.5 kJ/mol in the extreme cases) is also reasonable considering the errors involved in modeling. Further information regarding phase stability can also be gained in the discussion of ΔG in the next paragraph.

While ΔH may adequately approximate ΔG at low temperatures,²⁴ it is ΔG which determines the thermodynamic stability of solid phases at constant temperature. We have used the CALPHAD results discussed above to calculate ΔG vs x curves at 350 K (Fig. 9) to examine the relative phase stability, in particular, the fcc-bcc transition. As shown in this work, the thermodynamic equilibrium state, i.e., the coexistence of two terminal solid solutions, has not been established in ball-milled Fe-Cu. Instead, the system has been constrained to be single phase. We can therefore evaluate the ΔG functions of each phase to determine their relative stability. This point will be discussed further in the next paragraph. First, we note that the ΔG results provide an indication as to why, unlike for some other alloy systems, our ball milling experiments have not produced an amorphous phase. The liquid ΔG curve lies above those of solid phases. Even after considering free energy changes during undercooling,²⁴ the free energy of an undercooled liquid, which may be used to approximate the amorphous phase, will still have a significantly more positive ΔG than solid solutions. Second, as in the ΔH case, there is no crossover of the two curves for nonmagnetic alloys (dashed curves). Therefore, no thermodynamic transition between the fcc and bcc phases is predicted. In other words, the fcc phase would be more stable than the bcc phase throughout the entire composition range. Add-

ing the magnetic terms, based on Chuang's formulation,^{19,22} results in intersection of the two curves at approximately $x=60$ (Fig. 9). This is close to the two-phase transition region ($x=60-75$) observed in experiments. The small discrepancy may be a result of error in the CALPHAD fcc curve, which has been discussed in the preceding paragraph. Also, this intersection composition shifts to the Fe-rich side at higher temperature (the fcc phase will eventually become more stable than the bcc phase when the magnetic contribution disappears at higher temperatures). During ball milling, the effective temperature the powders have experienced may be somewhat higher than the value of 350 K we have estimated based on the vial temperature (about 310 K). We believe that, within our error, this intersection between the calculated ΔG curves is the cause for the observed fcc-bcc transition, and that thermodynamics determine phase formation in this system. In general, the present CALPHAD modeling and data for Fe-Cu solid solutions, with the incorporation of magnetic contributions, are satisfactory. They agree quantitatively well with the experimental ΔH data for the bcc phase, and semiquantitatively with the observed fcc-bcc transition. Further improvement is needed in the current CALPHAD data for the fcc phase to match experimental data. It is also obvious that more rigorous theoretical work is needed in order to better address this complex issue of describing thermodynamic functions for a magnetic system.

Finally, we note that the alloying of immiscible Fe and Cu presents a challenge to the current understanding of the ball-milling-induced alloying process, which has often been depicted as an interdiffusion reaction under kinetic constraints.²⁵ The dominant, positive enthalpy of mixing would preclude the presence of a driving force for such an interdiffusion reaction. Yet experiments yield the formation of single-phase supersaturated solid solution without reaching equilibrium. In our recent work on Zr-Al,²⁶⁻²⁸ we have used the term "polymorphous constraints" to describe the constraints that maintain the system as a single phase without reaching a two-phase stable or metastable equilibrium. This work followed discussions by other authors of polymorphous phase diagrams and polymorphous metastable phase formation under rapid quenching and vapor deposition.¹ In this respect, the ball-milled Zr-Al and Fe-Cu systems share the same characteristic, both demonstrating the presence of polymorphous constraints. We have suggested that the high interfacial energy associated with a fine-structured two-phase mixture is an important factor responsible for such polymorphous constraints.²⁶⁻²⁸

IV. CONCLUSIONS

We summarize the main conclusions of this work:

(1) Mechanical alloying can lead to the formation of extended solid solutions in immiscible systems such as Fe-Cu. The Fe-Cu alloys prepared by high-energy ball milling appear to have reproducible thermodynamic and structural properties.

(2) Solid solutions in the Fe-Cu system are characterized by a large positive enthalpy of formation. Their lattice

parameters exhibit rather strong positive deviation from those given by Vegard's law for an ideal solution.

(3) Mechanically alloyed Fe-Cu solid solutions are ferromagnetic, with saturation magnetization and Curie temperatures similar to those of vapor-deposited films. For the fcc solutions prepared by these two techniques, differences exist in the Curie temperatures and in the lattice parameters.

(4) Current CALPHAD modeling of the thermodynamic functions of metastable Fe-Cu solid solutions, with magnetic contributions incorporated, yields reasonable agreements with experimental determinations, in particular for the bcc solid solution. Some discrepancies exist for the Cu-rich fcc phase, suggesting deficiencies in the CALPHAD data.

(5) The large positive enthalpies of formation measured for the Fe-Cu solid solutions preclude the presence of a driving force for a simple isothermal interdiffusion reaction, a mechanism often invoked to explain alloying during ball milling. Polymorphous constraints prevent this system from reaching two-phase equilibrium during ball milling. Model calculations compared with experiments suggest that the observed bcc-fcc transition results from the relative thermodynamic stability of the two phases under polymorphous constraints.

ACKNOWLEDGMENTS

The authors thank Frank Brunner and Jaime Pagan for their assistance in sample preparation. This research is supported by NSF Grant DMR-9200932.

¹W. L. Johnson, *Prog. Mater. Sci.* **30**, 81 (1986).

²E. F. Kneller, *J. Appl. Phys.* **35**, 2210 (1964).

³K. Sumiyama and Y. Nakamura, in *Rapidly Quenched Metals*, edited by S. Steeb and H. Warlimont (Elsevier, Netherland, 1985), p. 859; *Acta Metall.* **33**, 1791 (1985).

⁴C. L. Chien, S. H. Liou, D. Kofalt, W. Yu, T. Egami, and T. R. McGuire, *Phys. Rev. B* **33**, 3247 (1986).

⁵L. J. Huang and B. X. Liu, *Appl. Phys. Lett.* **57**, 1401 (1990).

⁶P. H. Shingu, K. N. Ishihara, K. Uenishi, J. Kuyama, B. Huang, and S. Nasu, in *Solid State Powder Processing*, edited by A. H. Clauer and J. J. deBarbadillo (TMS, Warrendale, 1990), p. 21; K. Uenishi, K. F. Kobayashi, S. Nasu, H. Hatano, K. Ishihara, and P. H. Shingu, *Z. Metallkd.* **83**, 132 (1992).

⁷T. B. Massalski, Ed., *Binary Alloy Phase Diagrams* (ASM, Metals Park, OH, 1986), Vol. 1, p. 916.

⁸A. R. Miedema, *Philips Tech. Rev.* **36**, 217 (1976).

⁹C. C. Koch, in *Materials Science and Technology*, edited by R. W. Cahn, P. Haasen, and E. J. Kramer (VCH, Weinheim, 1991).

¹⁰J. Eckert, R. Birringer, J. C. Holzer, C. E. Krill III, and W. L. Johnson, *MRS Symp. Proc.* **238**, 739 (1992); *J. Appl. Phys.* **73**, 131, 2794 (1993).

¹¹R. A. Swalin, *Thermodynamics of Solids* (Wiley, New York, 1962), pp. 91-108.

¹²S. V. Vonsovskii, *Magnetism* (Wiley, New York, 1974), Vol. 2, p. 517.

¹³L. Kaufman and H. Beinstein, *Computer Calculations of Phase Diagrams* (Academic, New York, 1970).

¹⁴L. Kaufman and H. Nesor, *CALPHAD* **2**, 117 (1978).

¹⁵O. Kubaschewski, J. F. Smith, and D. M. Bailey, *Z. Metallkunde* **68**, 495 (1977).

¹⁶M. Hasebe and T. Nishizawa, *CALPHAD* **4**, 83 (1980).

¹⁷P. A. Linquist and B. Uhrenius, *ibid.*, p. 193.

¹⁸M. Hasebe and T. Nishizawa, *CALPHAD* **5**, 105 (1981).

¹⁹Y.-Y. Chuang, R. Schmid, and Y. A. Chang, *Metall. Trans. A* **15A**, 1921 (1984).

²⁰E. Hellstern, H. J. Fecht, Z. Fu, and W. L. Johnson, *J. Appl. Phys.* **65**, 305 (1989).

²¹J. Friedel, *Dislocations* (Pergamon, Oxford, 1964), pp. 448-457; M. Atzmon, K. M. Unruh, and W. L. Johnson, *J. Appl. Phys.* **58**, 3865 (1985).

²²Y.-Y. Chuang, R. Schmid, and Y. A. Chang, *Metall. Trans. A* **16A**, 153 (1985).

²³R. B. Schwarz, P. Nash, and D. Turnbull, *J. Mater. Res.* **2**, 456 (1987).

²⁴E. Ma and M. Atzmon, *J. Alloys Compounds* (in press).

²⁵L. Schultz, in *New Materials by Mechanical Alloying Techniques*, edited by E. Arzt and L. Schultz (Informationsgesellschaft, Berlin, 1989), p. 53.

²⁶E. Ma and M. Atzmon, *Phys. Rev. Lett.* **67**, 1126 (1991).

²⁷E. Ma and M. Atzmon, *Mater. Sci. Forum* **88-90**, 467 (1992).

²⁸E. Ma and M. Atzmon, *Mod. Phys. Lett. B* **6**, 127 (1992).